

# Tailoring a Biomaterial Structure Based on Poly(aspartic acid) and Poly(ethylene glycol)

LOREDANA ELENA NITA<sup>1</sup>, MANUELA TATIANA NISTOR (PINTILIE)<sup>1\*</sup>, AURICA P. CHIRIAC<sup>1</sup>

<sup>1</sup>„Petru Poni” Institute of Macromolecular Chemistry, 41 Grigore Ghica Vodă Alley, 700487, Iași, Romania

*Polymer complexation is one of the convenient routes for the development of new polymeric materials. Polymeric complex based on poly(aspartic acid) and poly(ethylene glycol) is an interesting compound due to its attractive properties brought by the both components. Poly(aspartic acid) belongs to the family of synthetic polypeptides and it is a biocompatible and biodegradable water-soluble polymer, and owing in part to the carboxylic groups has some similar chemical properties to that of poly(acrylic acid). Poly(ethylene glycol) is also an interesting nonionic polymer because it is soluble in water and several organic solvents, due to the presence of both hydrophobic and hydrophilic segments. The near-infrared chemical imaging (NIR-CI) method is the fusion between near-infrared spectroscopy and image analysis with the unique capability to provide both qualitative and quantitative data of localized and space-averaged chemical compositions. The NIR-CI technique is successfully used in pharmaceutical applications to reveal the extent of ingredient blending, particle size distribution, the presence of polymorphs, and trace contaminants. In the present study the homogeneity of the polymeric complex based on poly(aspartic acid) and poly(ethylene glycol) it was evaluated, using NIR-CI technique which was also sustained by zeta potential and FT-IR analyses, the methods being employed in order to characterize the compound as future potential biomaterial structure.*

*Keywords: biomaterial, poly(aspartic acid), poly(ethylene glycol), NIR-CI*

Complexation between polycarboxylic acids and nonionic proton-accepting polymers (Lewis polybases) via hydrogen-bonding interaction has attracted considerable attention [1, 2]. The research interest in this field has been further stimulated by potential applications of the hydrogen-bonding interpolymer complexes (IPCs) to various fields, such as drug delivery formulations [3, 4], biomaterials [5-8] surfactants [9, 10], membranes in separation technology [11-13].

The poly(aspartic acid) (PAS), belongs to the family of synthetic polypeptides and it is a biocompatible and biodegradable water-soluble polymer [14]. As biocompatible product it can be used in medicines, cosmetics, and food. It is also considered as sustainable and environmentally compatible chemical product. Its biodegradability makes it particularly valuable from the viewpoint of environmental acceptability and waste disposal. At the same time, no toxic or mutagenic effects have been reported for PAS [15].

Poly(ethylene glycol) (PEG) is a nonionic polymer soluble in both water and several organic solvents due to the presence of both hydrophobic and hydrophilic segments fact that makes it applicable for both industrial and biological applications [16]. The success of this polymer in biotechnology is explained through its mild action in cell components. PEG is also used as for drug delivery matrix and as coating to avoid immune responses to implants [17].

In the present paper, the interpenetration in aqueous solution of the macromolecular chains of poly(aspartic acid) and poly(ethylene glycol), it was investigated for a potential biomaterial structure. The interpolymer complexation process was evaluated by determining zeta potential, as well as by following the temperature influence on zeta potential and electrical conductivity for the prepared polymeric structure. The homogeneity of the polymeric

complex based on poly(aspartic acid) and poly(ethylene glycol) was estimated using near-infrared chemical imaging (NIR-CI) technique sustained by zeta potential and FT-IR analyses.

## Experimental part

### Materials and IPC preparation

Poly(aspartic acid) synthesis was described before [18, 20]. The obtained polymer PAS has  $M_w = 15,110$  and a polydispersity index of 1.317. Poly(ethylene glycol) ( $M_w = 10000$  Da) was purchased from Fluka Germany and used without further purification.

The complex PAS/PEG was prepared by direct mixing for 60 min of the stock aqueous solutions of the same concentrations - 1 g/dL - in different PAS/PEG ratios (% vol.): 0/100; 20/80; 50/50; 80/20 and 100/0. The total polymer concentration in the mixture was maintained constant during each experiment.

Water was purified using an Ultra Clear TWF UV System. The polymer mixtures in solution were then poured into Petri dishes in room conditions and films were obtained by casting.

### Methods and Equipment

#### Near infrared chemical imaging (NIR-CI)

NIR-CI investigation was made with the SPECIM'S Ltd. SisuCHEMA, as completely integrated Chemical Imaging Workstation. SisuCHEMA employs SPECIM's hyperspectral imaging technology in the NIR (1000-2500 nm) range. The SisuCHEMA system includes a Spectral Camera in the NIR range which provides between 320 and 640 pixel spatial resolution and image rate from 60 to 350 Hz. SisuCHEMA system includes Evince as powerful chemometric and image processing software package. With Evince the image data were processed and the spectral and spatial information were explored to classify and quantify the

\* email: [emapintilie@yahoo.com](mailto:emapintilie@yahoo.com); Tel: 0740907135

image content. The contrast in the chemical images were compared by methods using intensity of a single wavelength, peak-height ratio of two wavelengths, correlation coefficient with a reference spectrum and principal component analysis (PCA). The correlation coefficient method was also compared with partial least squares (PLS-DA) regression for further homogeneity investigations.

### Zeta potential estimation

Zeta Potential  $\zeta$  - was determined on a Malvern Zetasizer ZS (Malvern Instruments, UK) and the electrophoretic mobility ( $\mu$ ) was calculated with the Smoluchowski relationship:

$$\zeta = \eta\mu/\epsilon, \text{ and } \kappa\alpha \gg 1,$$

where:

$\eta$  - viscosity,  
 $\epsilon$  -dielectric constant,  
 $k$  and  $\alpha$  - Debye-Hückel parameter and particle radius.  
 $pH$  was adjusted at 7 with HCl or NaOH, with the Autotitrator Malvern MPT2 device.

The *electric conductivity* was determined on the same apparatus in parallel with zeta potential measurement. Each measurement was made 3 times and the average of the values is graphically represented.

*Hydrodynamic Diameter* – appreciated on the same equipment Malvern Zetasizer ZS, was determined applying the Stokes – Einstein relationship.

$$D_H = Kt / 3\pi\eta\Delta,$$

where:

$D_H$  - hydrodynamic diameter,  
 $k$  - Boltzman's constant,  
 $t$  - temperature,  
 $\eta$  - viscosity,  
 $\Delta$  - diffusion coefficient.

*FT-IR spectra* – the molecular structures via the bands identification from the *spectra* have been used (on a DIGILAB, Scimitar Series, USA, spectrophotometer; the resolution recording was 4  $cm^{-1}$ ).

### Results and discussion

#### NIR and FTIR spectra of the compounds

Figures 1a and 1b present the raw NIR spectra and the detail of neat PEG, PAS and PAS/PEG blends in the 1100 – 2500 nm regions. The bands due to the combination and first overtone bands of the CH stretching vibrations and that of the second overtone of the C-O stretching vibration appear both in PAS and PEG spectra. The spectral differences between PEG and PAS are more clearly evidenced in the 2100 – 2500 nm regions. Early work of Hilton [19] demonstrated the utility of the NIR region for measuring the absorption bands of the hydroxyl groups. OH groups are identified as the first overtone absorption at 1428 nm. The second and third overtones of the CH bands are the prominent bands at 2308 nm and 1735 nm. In case of PAS the prominent bands at 2480nm most likely belong to OH band. The above assignment leaves the peak at about 1800 nm as the CH stretch overtone [20]. Figures 1c and 1d illustrate FT-IR spectra in the 0 – 4500  $cm^{-1}$  regions

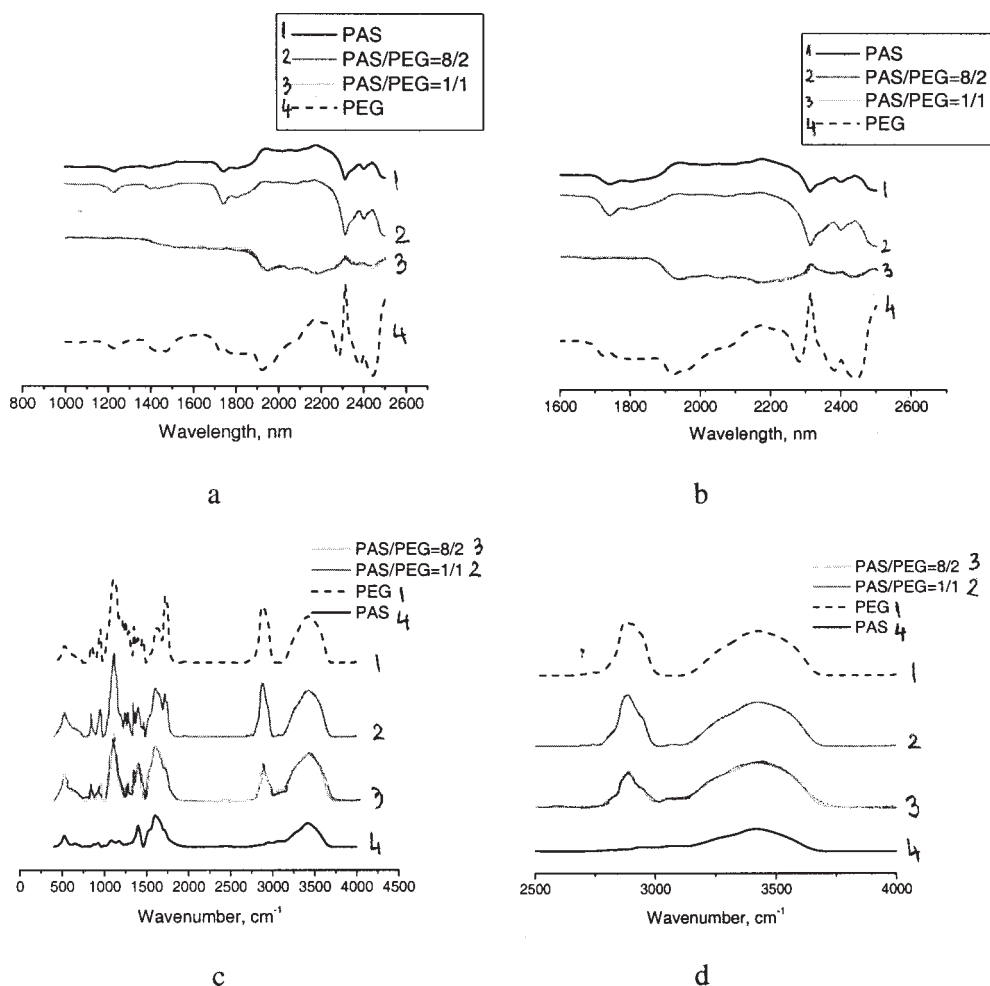


Fig. 1 NIR spectra: raw (a) and detail (b) and FTIR spectra: raw (c) and detail (d) of the compounds

and the detail from 2500 – 4000  $\text{cm}^{-1}$  region. The FT-IR spectrum of PAS is characterized by the presence of characteristic bands attributed to the stretching of different group vibrations. Thus, a broad band in the region of 1650 – 1720  $\text{cm}^{-1}$  is ascribed to the carbonyl stretching, meanwhile the broad strong bands between 3440 – 3424  $\text{cm}^{-1}$  match to the stretching vibrations of the intra-molecular hydrogen bond ( $\nu$  OH). The OH stretching vibration is observed in the region 3520-3330  $\text{cm}^{-1}$  exhibiting hydrogen bonded nature. PEG exhibits absorptions of a primary alcohol, comprising stretching and bending vibrations restricted to C-C stretch, C-O stretch, CH stretch (methylene absorptions) and the C-H bending. Similar bands are observed both in the NIR and FTIR spectra of complexes, but the bands appear at shifted positions confirming the complex formation.

#### Evaluation of homogeneity using statistical analysis by NIRCI

It is difficult to perform the evaluation of the distribution and prediction of the blend components simply by using the intensity at a fixed wavelength. Consequently, multivariate analysis is adopted from NIR-CI data. Near-infrared spectroscopy is the fusion between near-infrared spectroscopy and image analysis. Providing a chemical image the method can be used to visualize the spatial distribution of the chemical compounds in a sample. Each sample measurement generates a hyperspectral data cube containing thousands of spectra. An important part of a NIRCI analysis is the data processing of the hyperspectral data cube [21]. The conventional single point NIR spectroscopy measures a bulk average NIR spectrum and reflects an average composition of the sample [22]. NIR-CI adds spatial distribution information to the spectral information by combining traditional NIR spectroscopy with digital imaging. Translating the spectral signature from each pixel into, for example, chemical concentrations it is generated a set of chemical images that prove the distribution of each ingredient within the sample matrix. Moreover, NIR imaging enables quantitative information obtained without running separate calibration samples, since pure component spectra are directly available from the spectral imaging data cube of heterogeneously mixed samples [23]. This approach assures building a quantitative calibration model for pharmaceutical applications, for example in case of expensive peptide or protein drug formulations [24, 25].

Thus, with image analysis we create RGB (red-R, green-G, and blue-B) images from the data that originates from the image pixels of our structures (fig. 2). The spectral data was decomposed into a set of a small number of classification scores by PLS-DA. The scores of PLS-DA include the information of both the spectral variable and the response variable (the blending ratio). Therefore, we obtained the PLS-DA results having the correlation of both variables. Figure 3 displays the score images derived from PAS component class. In the score images, the pixels with higher and lower score values are indicated by white and dark colours, respectively. The colour in the most region of the score images is grey, the intermediate colour between white and dark colours. The predominantly grey score images indicate that the blends are relatively homogeneous. However, it is hard to discuss the quantitative degree of the homogeneity of these score images. Further quantitative results were obtained from PLS-DA analysis. Evince software enables to define classes of spectra to be used in a reference library, and one can perform PLS-DA calculations in both classification and

concentration modes. In the case of the classification mode, each library class is assumed to be pure component spectra from one chemical component and it has been automatically assigned a concentration of 1.0. The resulting PLS-DA model produces a classification “score” that (optimally) varies between 0 and 1. The score images, derived from PLS-DA and created from the predicted values of the spatially averaged contents of PAS and PEG in the blends, are summarized in table 1. These predicted values are very near to those of the polymeric blend contents.

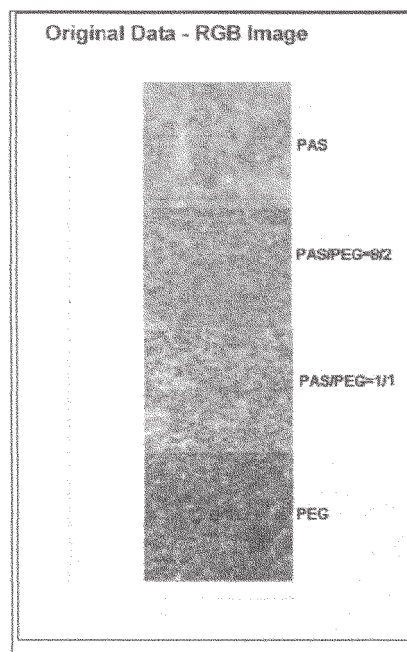


Fig.2. RGB Image

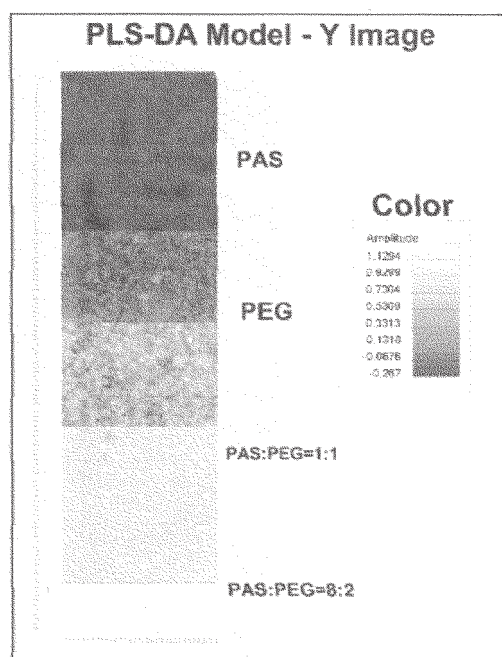


Fig.3. Score images of compounds

**Table 1**  
PREDICTED VALUES AND STD% OF PEG AND PAS COMPONENTS IN THE BLENDS

PAS/PEG [%]	Predicted values		STD%	
	PAS%	PEG%	PAS%	PEG%
50/50	57	43	9.076	9.056
80/20	88	12	5.483	5.479

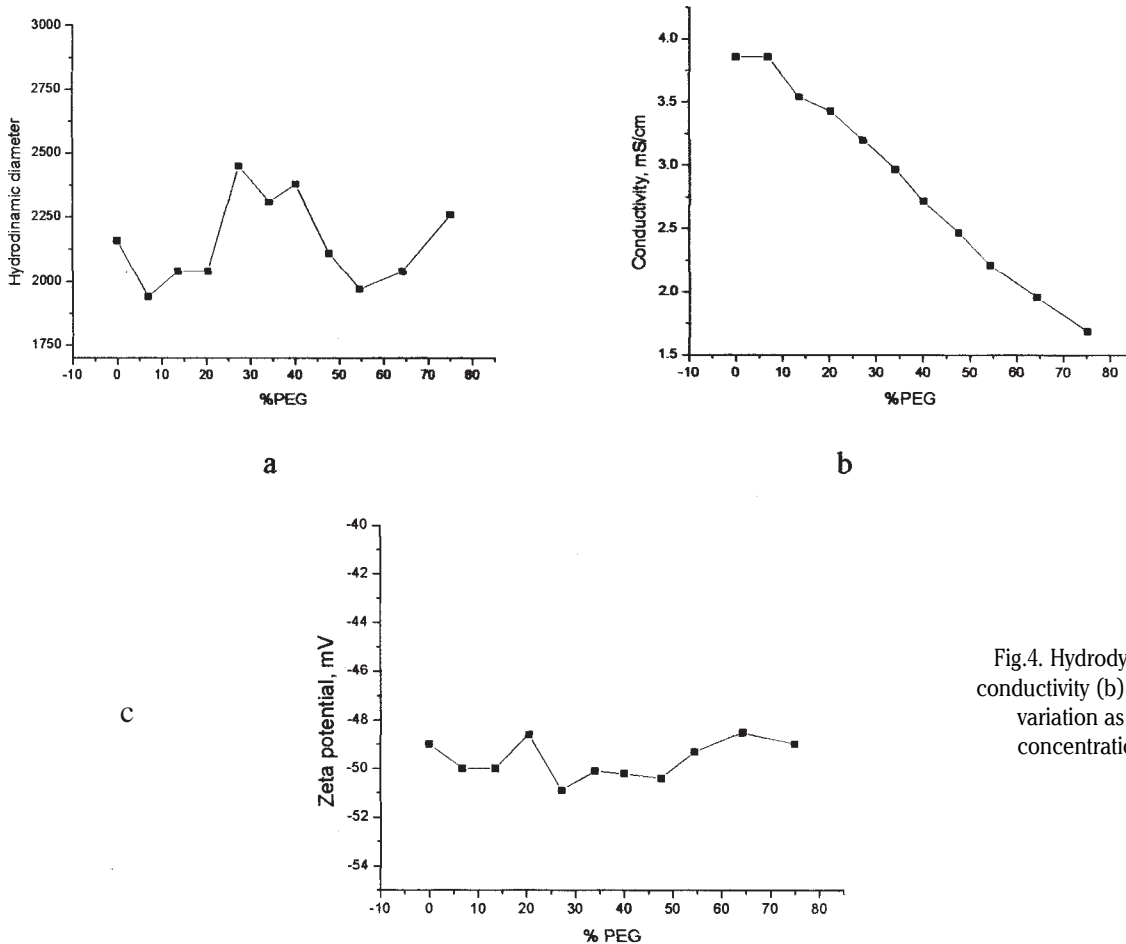


Fig.4. Hydrodynamic diameter (a), conductivity (b) and Zeta potential (c) variation as a function of PEG concentration in PAS solution

The small errors of the prediction explain the homogeneity of blends which is indicated by the standard deviation (STD) values also summarized in table 1. A well-mixed blend sample shows a normal distribution. Standard deviation (STD) is one of the useful parameters indicating the overall sample homogeneity and heterogeneity.

*Zeta potential, conductivity and hydrodynamic diameter analysis*

Because it reflects the effective charge on the particles and is therefore related to the electrostatic repulsion between them, zeta potential has proven to be extremely relevant to the practical study and control of colloidal stability and flocculation processes. For this reason in the next step it was studied the variation of  $\zeta$ , conductivity and hydrodynamic diameters (fig. 4 a-c) when the PEG was added in the solution of PAS. The study pursues evidencing the best ratio between PAS and PEG for their compatibility.

The formation of the compact interpolymer complexes in aqueous solutions from mixtures of such complementary polymers is done from successive hydrogen-bonding between the carboxylic groups of the polyacid and the proton acceptor groups of the polybase, which leads finally to interpolymer association [26].

The hydrodynamic diameter (fig. 4a) increases at 20 – 40% concentration of PEG. The inclusion of PEG evidences at the beginning the disturbance of the compacted structure of PAS with the appearance of some steric hindrance concretized in the increase of hydrodynamic diameter. After that growths of the hydrogen bonds have as effect the reducing of the hydrodynamic diameter. Normally, the conductivity decrease with the growths of the PEG content.

Zeta potential is relatively constant. These values attest the stability of the complex as well as of the homopolymers. Exception is the complex with 25% PEG

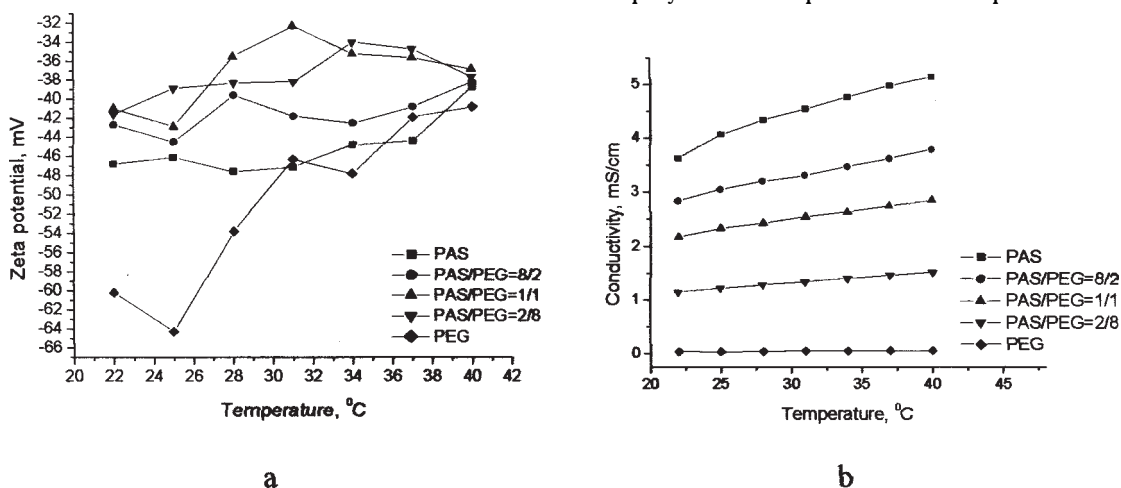


Fig. 5. Zeta potential (a) and conductivity (b) as function of temperature for the PAS/PEG

which presents a small increased of the zeta potential values.

However, because these interpolymeric complexes are made for biomedical purpose it was interesting to study the influence of the temperature on zeta potential and conductivity for blend in comparison with pure polymers. (figs. 5 a, b).

Zeta potential values of PAS/PEG blend are higher than of the homopolymers (fig. 5a), which indicates the stability of the interpolymeric complex with a new supramolecular structure with functional groups oriented on the surface. These observations are in agreement with the data of dynamic rheology presented elsewhere [27]. More than that, the absolute values of zeta potential at 37°C for PAS/PEG complexes are higher than 30 mV, which is considered an index of stability. So, the prepared interpolymeric complex presents a good stability allowing their use for biomedical purpose.

Since the conductivity is based on the movement of ions, it follows that the concentration of ions in the solution will have a great bearing on the assessment of ions in the solution. Therefore, conductivity it is used to indicate and estimate the degree of complexation between polymers in aqueous solution (fig. 5b). The interpolymeric complex has the value of the conductivity between the homopolymers, higher than PEG but lower than PAS.

## Conclusions

The homogeneity of the PAS/PEG interpolymeric complex was investigated by NIR-CI technique combined with multivariate data analysis. The homogeneity was confirmed by both qualitative and quantitative analysis. The score images directly depict the spatial distribution of interpolymeric complex components. The small STD values obtained from the histograms sustain the highly homogeneity of the interpolymeric complex.

The values of the zeta potential, the conductivity and the hydrodynamic diameters, evaluated during the preparation of the PAS/PEG interpolymeric complex, confirm the compatibility between the two polymeric components as well as the possibility to use the PAS/PEG blends for biomedical applications.

## Acknowledgements

*This work was supported by a CNCSIS-Idea Project, No 995: RESEARCHES IN THE FIELD OF POLYMERIC MATRICES DESIGN FOR SENSITIVE STRUCTURES Romania, Ministry of Education Research, 2009 – 2011.*

## References

1. BEKTUROV E. A., BIMENDINA L., Interpolymer Complexes, Adv. Polym. Sci., 43, 1980, p. 99
2. TSUCHIDA, E. ABE, K., Adv. Polym. Sci., 45, 1982, p. 111
3. OZEKI, T., YUASA, H., KANAYA, Y., J. Controlled Release, 63, 2000, p. 287
4. CARELLI V., DI COLO, G., NANNIPIERI E., POLI, B., SERAFINI, M. F., Int. J. Pharm., 202, 2000, p. 103
5. CHUN, M.-K., CHO, C.-S., CHOI, H.-K., J. Controlled Release, 81, 2002, p. 327
6. SULCA, N.M., LUNGU, A., POPESCU, R., GAREA, S. A., IOVU, H., Mat. Plast., 46, no. 1, 2009, p. 1
7. CARCEANU, I., COSMELEATA, G., GHIBAN, B., BALANESCU, M., NEDELICU, I., Mat. Plast., 44, no. 4, 2007, p. 321
8. CRACIUNESCU, O., LUNGU, M., ZARNESCU, O., GASPAR, A., MOLDOVAN, L., Mat. Plast., 45, no. 2, 2008, p. 163
9. VOROBEVA, G.A., GALTSEVA, E.V., KOZINTSEV, A.V., PROKOFEV, A.I., DUBINSKII, A.A., Russ. Chem. Bull. 47(11), 1998, p. 2155
10. MATHUR, A. M., DRESCHER, B., SCRANTON, A. B., KLIER, J., Nature, 392, 1998, p. 367
11. UMANA, E., OUGIZAWA, T., INOUE, T., J. Membr. Sci. 157, 1999, p. 85
12. SIVADASAN, K., SOMASUNDARAN, P., TURO; N.J., Coll. Polym. Sci., 269, 1991, p.131
13. PANAITESCU, D. M., NECHITA, P., IOVU, H., IORGA, M. -D., GHIUREA, M., SERBAN, D., Mat. Plast., 44, no. 3, 2007, p. 195
14. ROWETON, S., HUANG, S.-J., SWIFT, G., J. Environm. Polym. Degrad., 5(3), 1997, p. 175
15. NAKATO, T., TOSHITAKE, M., MATSUBARA, K., TOMIDA, M., KAKUCHI, T., Macromolecules, 31, 1998, p. 2107
16. GREENWALD R.B., Journal of Controlled Release 74, 2001, p. 159
17. ZALIPSKY, S. Bioconj. Chem. 6, 1995, p. 150
18. NEAMTU, I., CHIRIAC, A. P., NITA, L. E., BERCEA, M., J. Optoel. Adv.Mater. 9(11), 2007, p. 3459
19. HILTON, C.L., 31, 1959, p. 1610
20. SNAVELY, D., DUBSKY, J., J. Polym Sci: Part A, 34, 1996, p. 2575
21. RAYN, C., SKIBSTED, E., BRO, R., J of Pharm and Biomed Analysys, 48, 2008, p. 554
22. BELIZ, K., DINÇ, E., BALEANU, D., Rev. Chim.(Bucuresti), 60, no. 6, 2009, p. 544
23. DINÇ, E., BALEANU, D., Rev. Chim.(Bucuresti), 60, no. 3, 2009, p. 216
24. CIURCZAK, E.W., DRENNEN, J.K., III (Eds.), Marcel Dekker Inc., New York, 2002
25. REICH, G., Advanced Drug Delivery Reviews, 57, 2005, p. 1109
26. SIVADASAN, K., SOMASUNDARAN, P., TURO, N.J. Coll. Polym. Sci., 269, 1991, p.131
27. CHIRIAC, A.P., NITA, L., NEAMTU, I., BERCEA, M., PINTILIE, M.-T., Colloids and Surfaces A: Physicochemical and Engineering Aspects, 348, 2009, p. 254

Manuscript received: 16.09.2009